High Power Laser Science and Engineering, (2024), Vol. 12, e89, 5 pages.
doi:10.1017/hpl.2024.74

HIGH POWER LASER SCIENCE AND ENGINEERING

RESEARCH ARTICLE

Long-term stable timing fluctuation correction for a picosecond laser with attosecond-level accuracy

Hongyang Li[1,2,3], Keyang Liu[4], Ye Tian[2,3], and Liwei Song[2,3]

[1] *School of Physics Science and Engineering, Tongji University, Shanghai, China*

[2] *State Key Laboratory of High Field Laser Physics, Shanghai Institute of Optics and Fine Mechanics, Chinese Academy of Sciences, Shanghai, China*

[3] *Center of Materials Science and Optoelectronics Engineering, University of Chinese Academy of Sciences, Beijing, China*

[4] *XIOPM Center for Attosecond Science and Technology, State Key Laboratory of Transient Optics and Photonics, Xi'an Institute of Optics and Precision Mechanics, Chinese Academy of Sciences, Xi'an, China*

(Received 26 July 2024; revised 12 October 2024; accepted 17 October 2024)

Abstract

Rapid advancements in high-energy ultrafast lasers and free electron lasers have made it possible to obtain extreme physical conditions in the laboratory, which lays the foundation for investigating the interaction between light and matter and probing ultrafast dynamic processes. High temporal resolution is a prerequisite for realizing the value of these large-scale facilities. Here, we propose a new method that has the potential to enable the various subsystems of large scientific facilities to work together well, and the measurement accuracy and synchronization precision of timing jitter are greatly improved by combining a balanced optical cross-correlator (BOC) with near-field interferometry technology. Initially, we compressed a 0.8 ps laser pulse to 95 fs, which not only improved the measurement accuracy by 3.6 times but also increased the BOC synchronization precision from 8.3 fs root-mean-square (RMS) to 1.12 fs RMS. Subsequently, we successfully compensated the phase drift between the laser pulses to 189 as RMS by using the BOC for pre-correction and near-field interferometry technology for fine compensation. This method realizes the measurement and correction of the timing jitter of ps-level lasers with as-level accuracy, and has the potential to promote ultrafast dynamics detection and pump–probe experiments.

Keywords: laser interferometry; optical cross-correlator; ultrafast laser pulse synchronization

1. Introduction

With the development of laser technology, the peak power of laser pulses has been increased to terawatt, petawatt or even exawatt levels[1–3], which has promoted the progress of high-field ultrafast laser science by driving particle acceleration[4–6], secondary radiation such as electromagnetic pulses emission[7], terahertz systems[8–10], quasiparticles emission[11], and extreme electric and magnetic fields excitation[12,13]. On the other hand, free electron lasers (FELs) have been proven excellent detection light sources due to their wide and continuously adjustable spectral coverage, high beam quality and short pulse duration[14]. Recently, researchers have successfully performed attosecond pump–probe experiments and explored the application of this novel technique in ionization dynamics[15]. High-precision time synchronization is the key factor for successful implementation of ultrafast pump–probe experiments, which have been performed more and more frequently on laser facilities and FELs. Reducing the timing jitter between laser pulses is invaluable for enhancing the performance of lasers, thus achieving efficient and stable operation in areas such as precise measurement and high-field ultrafast laser physics. In scientific research projects that involve large-scale time synchronization, such as FELs and particle accelerators, the active correction of timing jitter plays a crucial role[16]. By precisely correcting timing jitter, it is possible to ensure that all systems achieve accurate collaborative operation, thereby liberating the full value of large-scale scientific facilities. Furthermore, for applications related to the laser field, such as the generation of high harmonics[17] and attosecond pulses[18], optical

Correspondence to: Y. Tian and L. Song, State Key Laboratory of High Field Laser Physics, Shanghai Institute of Optics and Fine Mechanics, Chinese Academy of Sciences, Shanghai 201800, China. Emails: tianye@siom.ac.cn (Y. Tian); slw@siom.ac.cn (L. Song)

phase-locked electron emission[5] and attosecond electron pulse generation[19], the timing jitter needs to be controlled within one optical cycle, that is, at the attosecond level.

The balanced optical cross-correlator (BOC), which was introduced in 2003[20], has played a pivotal role in the synchronization of laser envelopes with its unique advantages and has shown broad application prospects in practical applications. In 2022, Yang *et al.*[21] characterized the timing jitter of a self-made high-repetition-rate solid-state fiber laser, which had a pulse train timing jitter root-mean-square (RMS) of 130 as using the BOC technology. To prevent signal distortion or errors caused by time deviation and maintain excellent accuracy and stability during transmission, precise measurement and control of timing jitter are necessary. In 2024, Wu *et al.*[22] combined a novel heterodyne method with BOC technology to determine the out-of-loop timing jitter performance of a free-running Ti:sapphire laser, with out-of-loop integrated timing jitter of 11.9 as from 10 kHz to the Nyquist frequency (50 MHz). Interferometry, as an excellent measurement technology that utilizes the coherence of lasers to measure phase fluctuation, can also capture extremely minuscule timing jitters by analyzing changes in interference patterns. In 2013, Chosrowjan *et al.*[23] demonstrated using coherent beam combining technology in high-power multi-channel amplifier systems to increase pulse power as a proof of principle, and utilized the near-field interference method to compensate for the timing jitter of the optical phase introduced by laser systems, realizing RMS timing jitter control of approximately $\lambda/25$. In 2020, Liu *et al.*[24] proposed double-humped spectral beam interferometry to simultaneously measure the absolute time delay and the relative time delay, and the RMS deviation of approximately 70 as was achieved.

The aforementioned methods for measuring and controlling noise and timing jitter either require identical lasers or are tailored specifically for femtosecond lasers with short propagation distances. These approaches not only necessitate costly equipment, but also fail to convincingly demonstrate their applicability and scalability in large-scale laser systems. Precise control of both noise and timing jitter is necessary for large laser systems operated in complex and ever-changing environments. Therefore, the development of a method to measure and correct the timing jitter of the pulse trains that have longer duration and longer propagation distances is essential to ensure the stability and reliability of laser systems in high-precision experiments and applications.

In this article, we introduce a synchronization technology that combines the BOC and interferometry measurement to characterize the time fluctuation of the laser pulse envelope and phase. With time-delay feedback loops, the time drift between picosecond laser pulses is compensated to 189 as ($\lambda/18$). Benefiting from the advantages of the BOC in terms of large correction range and interferometry in phase sensitivity, this technology offers strong anti-interference ability and high measurement accuracy. Fine compensation of timing fluctuation provides a basis for pump–probe experiments of attosecond accuracy and phase sensitivity.

2. Experimental setup, results and analysis

The experimental setup is shown in Figure 1. The system is driven by a Yb:yttrium aluminum garnet (YAG) laser with 0.8 ps pulse duration, 740 μJ pulse energy and 1030 nm center wavelength. The BOC technology is adopted to characterize the time fluctuation. The cross-correlation intensity of BOC measurement has a linear characteristic within a specific delay range, which is attributed to the overlap of two laser pulses in time. It is worth noting that the slope of the linear region represents the measurement accuracy. A shorter pulse duration makes it easier to acquire

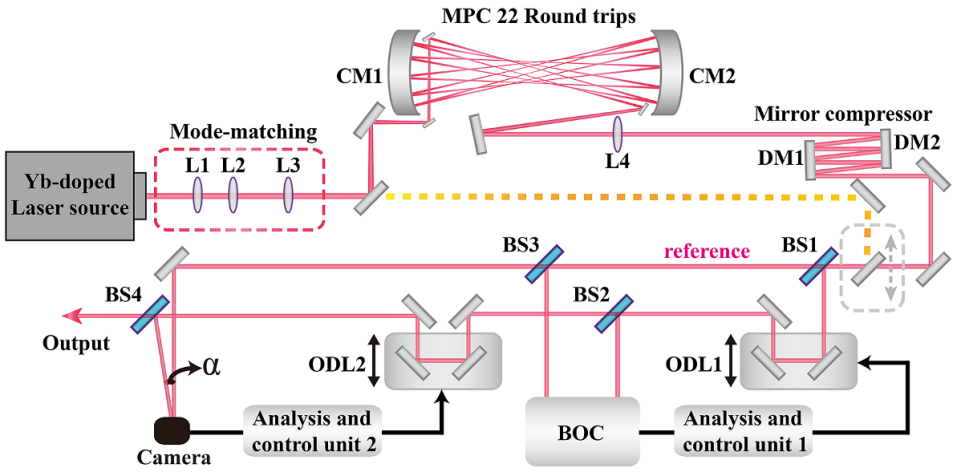

Figure 1. Schematic illustration of the experimental setup. BS1–BS4, beam splitters; L1–L4, lenses; CM1 and CM2, curved mirrors; MPC, multi-pass cavity; DM1 and DM2, dispersive mirrors; ODL1 and ODL2, optical delay lines.

https://doi.org/10.1017/hpl.2024.74 Published online by Cambridge University Press

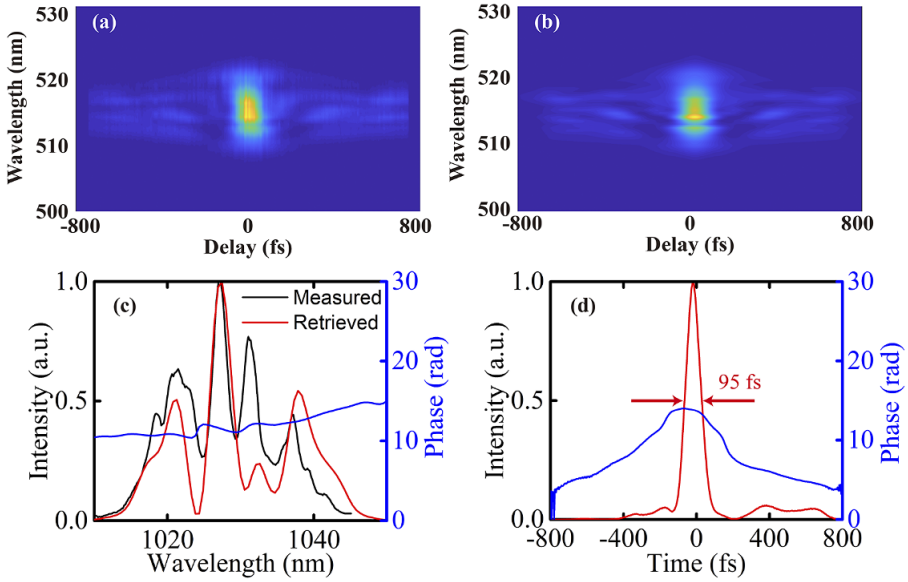

Figure 2. Temporal characterization after compression. (a) Measured FROG traces. (b) Retrieved FROG traces. (c) Retrieved spectrum (red line) and phase (blue line) together with the measured spectrum (black line). (d) Temporal intensity (red line) and phase (blue line).

steep slopes and improves measurement accuracy[25]. Thus, further compressing the laser pulse duration is an effective way to increase measurement accuracy.

A Herriott-type multi-pass cavity (MPC) is employed for pulse duration compression, as depicted in Figure 1. It is made up of two concave mirrors with a 600-mm curvature radius and 2-inch diameter. The MPC is built in atmosphere, and air is used as the nonlinear medium. Taking into account the ionization threshold of air and the safe operation zone of the MPC, the pulse energy is set to 650 μJ and the distance between cavity mirrors is 750 mm. The spectrum is continuously broadened due to self-phase modulation (SPM) when the laser pulse performs 22 round trips in the MPC, equating to a distance of 33 m in the air. The dispersion is compensated by a pair of dispersive mirrors, which offer a dispersion of $-12{,}000$ fs^2.

The pulse temporal profile is characterized by a second harmonic generation frequency-resolved optical gating (SHG-FROG), as shown in Figure 2. The measured and retrieved FROG traces are shown in Figures 2(a) and 2(b) with a FROG error of 0.9%. As shown in Figure 2(c), the measured (black line) and retrieved (red line) spectra are in good agreement. The pulse duration at full width at half-maximum (FWHM) is 95 fs, as shown in Figure 2(d). The output pulse energy is 590 μJ, yielding about 90% transmission efficiency.

The compressed laser pulses are split by a beam splitter (BS1) and imported into different paths. After approximately 10 m of propagation, the timing fluctuation can arise from several factors, with the major contributions typically being atmospheric turbulence, mechanical vibrations of the mirror holders and thermal drift caused by environmental temperature. Environmental temperature, in particular, is a significant source of timing errors, as the refractive index of air varies with temperature, leading to changes in the optical path length. Mechanical vibrations are also important, as even minor displacements of optical elements can alter the optical path length and introduce timing jitter. While atmospheric turbulence also plays a role, ensuring mechanical stability and a constant temperature environment is often the main concern in minimizing timing errors. Therefore, the timing fluctuation needs to be actively compensated through feedback control systems. Subsequently, the beams are reflected by BS2 and BS3 into a BOC for time fluctuation measurement. In addition, the BOC signal is analyzed to control a feedback loop for the synchronization of pulse envelopes.

Figure 3(a) depicts the detailed setup of the noncollinear BOC. A 50:50 beam splitter splits the incident laser pulses into two arms of the BOC. The laser beams are focused noncollinearly on 0.5-mm-thick type-I ($\theta = 23.4°, \varphi = 0°$) beta barium borate (BBO) crystals for sum frequency generation (SFG). The noncollinear setup eliminates the influence of second harmonics. A glass plate is inserted into one of the transmitted beams for the reference of time offset. The SFG signals are subtracted by a balanced photodetector (PDB450, Thorlabs Inc.) to characterize the timing jitter. Measurement error caused by energy drift is significantly reduced by balanced detection.

To compare the BOC measurement accuracy for long and short pulses, the cross-correlation 'S' curves are measured with and without pulse duration compression (yellow dashed lines in Figure 1), as shown in Figure 3(b). The corresponding accuracy is 14.57 mV/fs (0.8 ps) and 52.5 mV/fs (95 fs),

https://doi.org/10.1017/hpl.2024.74 Published online by Cambridge University Press

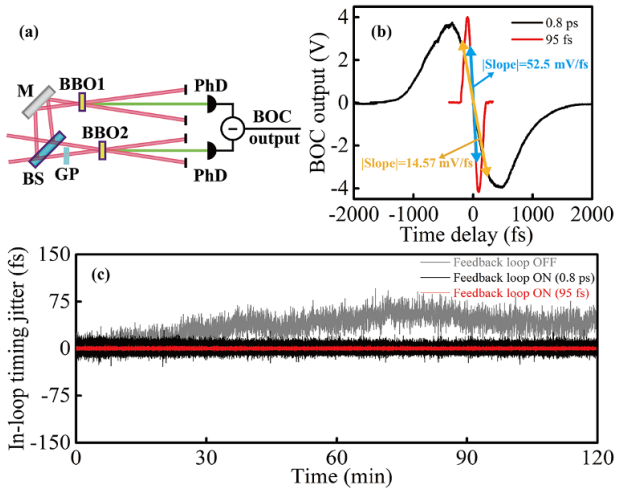

Figure 3. (a) Schematic of the noncollinear BOC. M, mirror; BS, beam splitter; GP, glass plate; BBO1 and BBO2, beta barium borate crystals; PhD, photodetector. (b) Measured cross-correlation curves at 0.8 ps and 95 fs, respectively. (c) Timing drift of 0.8 ps when the feedback loop is off (gray line) and on (black line) together with the timing drift of 95 fs when the feedback loop is on (red line).

which indicates a 3.6 times improvement in measurement accuracy by compressing the laser pulse duration from 0.8 ps to 95 fs via an MPC compressor. Analysis control unit 1 includes a data acquisition card, which captures the voltage amplitude output from the balanced photodetector and converts it into timing jitter using the measurement accuracy, thus determining the required movement distance for ODL1. This process forms a closed-loop feedback system. The time fluctuation is corrected by the feedback loop, in which the BOC signal is analyzed and a delay line with 10 nm accuracy is controlled to compensate for the drift. As shown in Figure 3(c), with higher measurement accuracy, the corrected time fluctuation decreases from 8.3 to 1.12 fs RMS in 2 hours, which is shorter than one optical cycle.

On this basis of the BOC-based feedback loop, interferometry-based feedback is applied to further improve the timing accuracy to attosecond level and realize phase synchronization between laser pulses. Interferometry benefits high precision in phase measurement by converting the fluctuation of interference fringes to relative phase drift. Assume that a laser propagates along the z-axis, which is perpendicular to the plane formed by the x-axis (horizontal direction) and the y-axis (vertical direction). The horizontal spatial electric field distribution of the laser when it is incident at a certain angle on the laser beam profiler can be written as follows[24,26]:

$$E(x) = A(x)\exp\left[j\left(kx+\phi\right)\right], \tag{1}$$

where $A(x)$, k and ϕ represent the amplitude, wave vector and phase of the laser on the x-axis, respectively. When laser

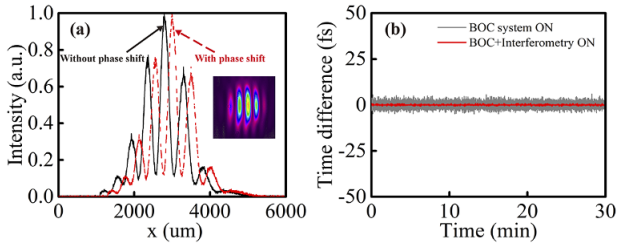

Figure 4. (a) Schematic diagram of interference fringe intensity distribution with (red line) and without (black line) phase drift (inset shows the coherently combined). (b) Time difference when the BOC system is ON and when both BOC and interferometry are ON.

beams are incident on a camera with a small included angle, the intensity of interference fringes is as follows:

$$I(x) = \sum A_n(x)^2 + 2\sum_n \sum_{m,m\neq n} A_n(x)A_m(x) \cdot \cos\left[2\pi\alpha x/\lambda + (\phi_n - \phi_m)\right], \tag{2}$$

where λ is the laser wavelength, $\Delta\varphi = 2\pi\alpha x/\lambda + (\phi_n - \phi_m)$ is the laser phase difference and α is the angle between the two incident lasers beams. The interference period $D = \lambda/\sin\alpha$. The optical path difference $\delta = d \times \sin\alpha$, where d is the movement distance of the interference fringes[24]. Thus, the timing jitter is converted to the movement distance of the interference fringes.

As in the experimental setup shown in Figure 1, the transmissions of BS2 and BS3 are reflected onto a camera (Ophir-Spiricon, BeamGage) with a small included angle to record interference fringes. The fringes are analyzed by analysis and control unit 2, which also includes data acquisition and processing cards, captures the interference fringe data output from the camera and calculates the movement distance d of the fringes between consecutive moments, and optical delay line 2 is controlled to compensate for the laser phase drift.

The interference fringes are shown in Figure 4(a) with a beam pattern as the insert. Phase shift between laser pulses is characterized by the offset of interference fringes, as indicated by the red dotted line in Figure 4(a). The shift of interference fringes is converted to optical path difference by $\delta = d \times \sin\alpha$. The included angle $\alpha = 0.13°$ is calculated by an interference period of 439 μm. By fine adjustment of the interferometry-based feedback loop, the time fluctuation is compensated to 189 as RMS over 30 minutes, which represents $\lambda/18$ for a laser wavelength of 1030 nm, as shown in Figure 4(b).

In the closed-loop feedback system, feedback bandwidth plays a vital role in ensuring that the system operates accurately, stably and efficiently. The feedback bandwidth mainly depends on the performance of a series of components in the experiment, including the photodetector, data acquisition card, camera acquisition frequency,

https://doi.org/10.1017/hpl.2024.74 Published online by Cambridge University Press

proportional–integral–derivative (PID) algorithm and the response speed of the motor. Limited by the stepper motor speed and camera acquisition speed, the feedback bandwidth is 1 kHz and 10 Hz in the BOC and interferometry-based feedback loops, respectively. The bandwidth can potentially be further increased by improving the speed of the detection. Furthermore, owing to the features of the optical delay line, the timing jitter can be compensated for up to 66.7 as, which ultimately determines the best compensation effect that the synchronization system can achieve. The timing jitter compensation capabilities can be further enhanced in the future by further compressing the pulse duration as well as improving the feedback bandwidth.

3. Conclusions

In conclusion, we demonstrate a mixed BOC and interferometry approach for active correction of the timing jitter to the attosecond level. This method combines the advantages of both, exhibiting robust anti-interference properties and providing large-scale correction and fine compensation of timing jitter. By compressing the pulse duration from 0.8 ps to 95 fs with an MPC compressor, the timing measurement accuracy is improved by a factor of approximately 3.6. In addition, the synchronization accuracy is increased from 8.3 to 1.12 fs RMS. On this basis, an interferometry-based feedback loop is used to compensate for the phase fluctuation to 189 as ($\lambda/18$) RMS. As a result, it would be a valuable scientific exploration to combine the BOC with interferometry technology to achieve ultrafast optical-to-optical synchronization with attosecond-level accuracy. The technology not only demonstrates extraordinary performance and synchronization accuracy, but also opens up a new route for active synchronization of large-scale scientific facilities and FELs.

Acknowledgements

This work was supported by the National Natural Science Foundation of China (Nos. 12325409, 12388102 and U23A6002), the CAS Project for Young Scientists in Basic Research (No. YSBR-059), the Zhangjiang Laboratory Construction and Operation Project (No. 20DZ2210300) and the Shanghai Pilot Program for Basic Research – Chinese Academy of Sciences, Shanghai Branch.

References

1. C. N. Danson, C. Haefner, J. Bromage, T. Butcher, J.-C. F. Chanteloup, E. A. Chowdhury, A. Galvanauskas, L. A. Gizzi, J. Hein, D. I. Hillier, and J. D. Zuegel, High Power Laser Sci. Eng. **7**, e54 (2019).
2. Z. Y. Li, Y. X. Leng, and R. X. Li, Laser Photonics Rev. **17**, 2100705 (2023).
3. Z. Y. Li, Y. Kato, and J. Kawanaka, Sci. Rep. **11**, 151 (2021).
4. T. Esirkepov, M. Yamagiwa, and T. Tajima, Phys. Rev. Lett. **96**, 105001 (2006).
5. Y. Tian, J. S. Liu, W. T. Wang, C. Wang, A. H. Deng, C. Q. Xia, W. T. Li, L. H. Cao, H. Y. Lu, H. Zhang, Y. Xu, Y. X. Leng, R. X. Li, and Z. Z. Xu, Phys. Rev. Lett. **109**, 115002 (2012).
6. M. Thévenet, A. Leblanc, S. Kahaly, H. Vincenti, A. Vernier, F. Quéré, and J. Faure, Nat. Phys. **12**, 355 (2016).
7. R. Qi, C. L. Zhou, Z. R. Zheng, D. D. Zhang, X. J. Yang, J. Y. Gui, L. W. Song, Y. Tian, and R. X. Li, Opt. Express **32**, 2670 (2024).
8. Y. S. Zeng, C. L. Zhou, L. W. Song, X. M. Lu, Z. P. Li, Y. Y. Ding, Y. F. Bai, Y. Xu, Y. X. Leng, and Y. Tian, Opt. Express **28**, 15258 (2020).
9. Y. Tian, J. S. Liu, Y. F. Bai, S. Y. Zhou, H. Y. Sun, W. W. Liu, J. Y. Zhao, R. X. Li, and Z. Z. Xu, Nat. Photonics **11**, 242 (2017).
10. D. D. Zhang, Y. F. Bai, Y. S. Zeng, Y. Y. Ding, Z. P. Li, C. L. Zhou, Y. X. Leng, L. W. Song, Y. Tian, and R. X. Li, IEEE Photonics J. **14**, 5910605 (2022).
11. D. D. Zhang, Y. S. Zeng, Y. F. Bai, Z. P. Li, Y. Tian, and R. X. Li, Nature **611**, 55 (2022).
12. H. Hamster, A. Sullivan, S. Gordon, W. White, and R. Falcone, Phys. Rev. Lett. **71**, 2725 (1993).
13. S. Y. Zhou, Y. F. Bai, Y. Tian, H. Y. Sun, L. H. Cao, and J. S. Liu, Phys. Rev. Lett. **121**, 255002 (2018).
14. D. D. Zhang, Y. S. Zeng, Y. Tian, and R. X. Li, Photon. Insights **2**, R07 (2023).
15. Z. H. Guo, T. Driver, S. Beauvarlet, D. Cesar, J. Duris, P. L. Franz, O. Alexander, D. Bohler, C. Bostedt, and A. Marinelli, Nat. Photonics **18**, 691 (2024).
16. M. Xin, K. Şafak, and F. X. Kärtner, Optica **5**, 1564 (2018).
17. P. B. Corkum, Phys. Rev. Lett. **71**, 1994 (1993).
18. F. Krausz and M. Ivanov, Rev. Mod. Phys. **81**, 163 (2009).
19. C. L. Zhou, Y. F. Bai, L. W. Song, Y. S. Zeng, Y. Xu, D. D. Zhang, X. M. Lu, Y. X. Leng, J. S. Liu, Y. Tian, R. X. Li, and Z. Z. Xu, Nat. Photonics **15**, 216 (2021).
20. R. T. Schibli, J. Kim, O. Kuzucu, T. J. Gopinath, N. S. Tandon, S. G. Petrich, A. L. Kolodziejski, G. J. Fujimoto, P. E. Ippen, and X. F. Kaertner, Opt. Lett. **28**, 947 (2003).
21. R. A. Yang, M. H. Zhao, X. G. Jin, Q. Li, Z. Y. Chen, A. M. Wang, and Z. G. Zhang, Optica **9**, 874 (2022).
22. H. T. Wu, H. Xu, and J. Y. Zhao, Opt. Lett. **49**, 742 (2024).
23. H. Chosrowjan, H. Furuse, M. Fujita, Y. Izawa, J. Kawanaka, N. Miyanaga, K. Hamamoto, and T. Yamada, Opt. Lett. **38**, 1277 (2013).
24. K. Y. Liu, L. W. Song, Y. Q. Liu, X. L. Wang, Z. Y. Huang, Y. H. Tang, X. B. Wang, Z. Z. Liu, and Y. X. Leng, Opt. Express **28**, 35498 (2020).
25. H. S. Shi, Y. J. Song, C. Y. Wang, L. M. Zhao, and M. L. Hu, Opt. Lett. **43**, 1623 (2018).
26. R. Q. Liu, C. Peng, W. S. Wu, X. Y. Liang, and R. X. Li, Opt. Express **26**, 2045 (2018).

https://doi.org/10.1017/hpl.2024.74 Published online by Cambridge University Press